

Laser micro sintering – a quality leap through improvement of powder packing

A. Streek, P. Regenfuss, R. Ebert, H. Exner

Laserapplikationszentrum, Fachbereich MPI, Hochschule Mittweida

Mittweida

D-09648

streek@htwm.de

Reviewed, accepted September 10, 2008

Keywords

Laser micro sintering, metals, generation, powder, density

Abstract

Laser micro sintering, a modification of selective laser sintering for freeform fabrication of micro-parts, was continuously upgraded since its first application. Poor density of the powder layers has been a persisting problem that had to be dealt with from the beginning. One solution was the application of high intensity q-switched laser pulses. Compaction of the material and improvement of the sinter resolution was achieved. But with these pulse-regimes only limited density of the sintered body has been achievable. Recently special efforts have been made to get rid of or at least reduce these drawbacks by markedly higher compaction of the respective powder layers. There is clear evidence that with sufficiently compacted powder layers even laser micro sintering with continuous radiation should be feasible. Till recently laser sintering of metal had been applied mainly to produce monolithic components. With the upgraded technique direct generation of micro devices with freely movable subassemblies can be possible.

Introduction

In the year 2002 selective laser micro sintering was developed by Laserinstitut Mittelsachsen e.V. [1]. It is a modification of selective laser sintering and has been successfully employed since then to generate metal micro parts. State of the art was the generation of micro parts, with effects of q-switched laser pulses. The implementation of a q-switched sintering regime was the consequence of the poor control of the powder coating. With this procedure, the selective sintering of thin and irregular powder layers with a low packing density was reasonably reliable. The detrimental effects of q-switched pulses was the poor density of the resulting specimens of around 60-70%, compared to the specific mass of the material, and the relatively large radius of the collaterally fused zone.

Since 2005, new powder coating techniques have been tested to improve the powder layer density. A variety of different rakes has been experimented with among others the approved ring shaped blade [2] has been supplied with compressing rollers, and additional force supported rakes have been tested to achieve denser powder packings. Higher density seems not possible by upgrading the mechanical components of the powder coating system. A new idea of powder packing is the compaction of the powder layer by pressure previous to laser sintering, as in the familiar technique of pressure injection molding.

Features of the recent laser micro sintering

The powders that are used for laser micro sintering have grain diameters of a few micrometers and below. Therefore they settle to only very poor densities of around 20%. Powders with grain sizes around 50 μm -100 μm , used in conventional laser sintering, have densities of 50% and more. Early experiments in 2002 showed that with sintering of sub-micrometer powders by continuous laser radiation the melt phase contracted to isolated small spheres instead of fusing with the underlying layer or the substrate [Fig. 1].

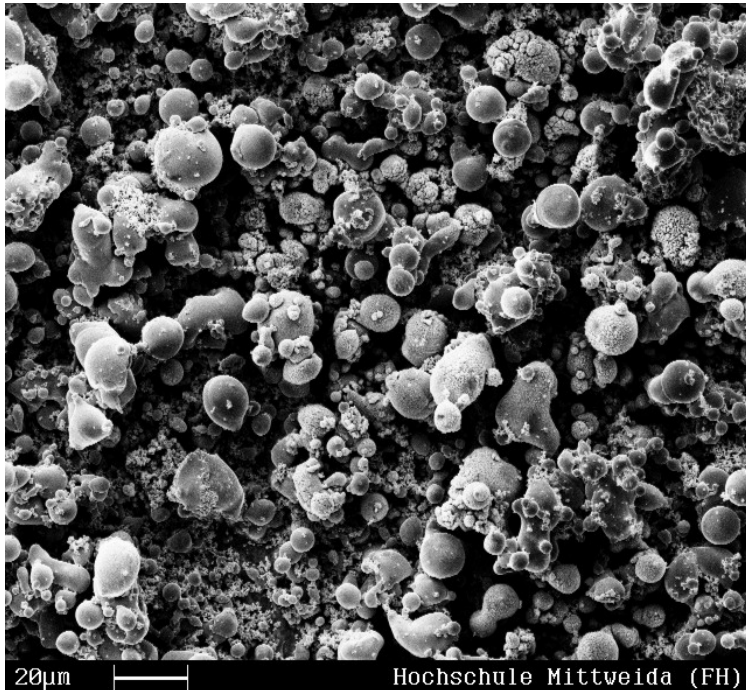


Fig. 1: 'Balling' of sub-micrometer tungsten powder upon irradiation with a continuous 1064nm laser beam

One solution for selective laser sintering of thin and fluffy powder layers with the underground body was the application of short and intensive pulses, obtained with a q-switched laser. The crucial effect of those pulses next to a comparably short life time of the involved liquid phase is the plasma shock wave arising from the excitation of initially evaporated material. The shock wave suppresses eruption of the generated melt pool and forces the liquid material downward. This effect has been reported as "the condensing effect" of the q-switched regime [3]. Other authors emphasize the recoil caused by boiling as the flattening effect in laser sintering by. [4,5]

After the breakdown of the shockwave boiling of the melt pool

may take place [Fig. 2] if the material has not lost its excess heat by the induced fusion with its substrate body.

One can assume that the irradiation time of the probe is shorter than the actual pulse-length due to the cut-off of the laser-beam by plasma [6] which is a familiar phenomenon known as 'plasma-shielding'.

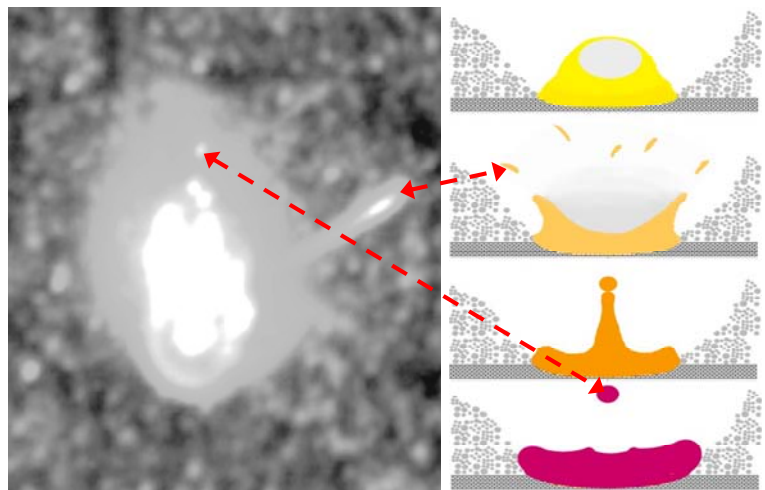


Fig. 2: Photograph (exposure: 1ms) of a pulse event with terminatory boiling of the melt.

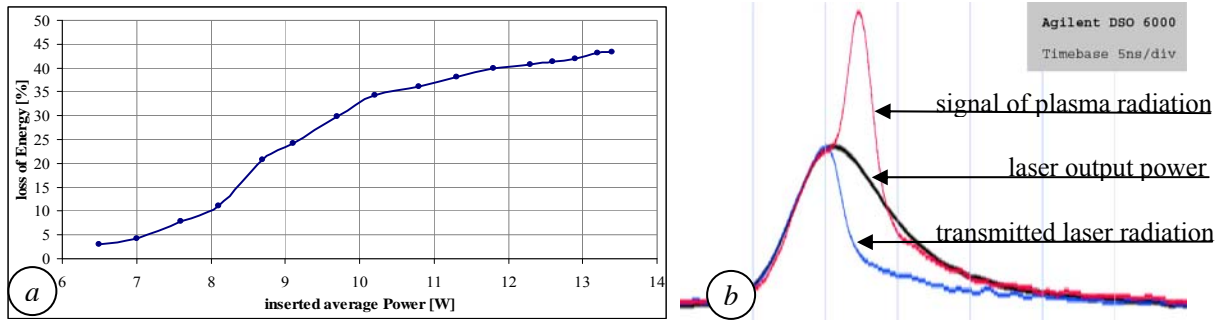


Fig. 3: Self attenuation of focused 1064nm laser pulses by the plasma generated from “air-breakthrough”. The intensity in the beam waist was in the order of $5 \cdot 10^{19} \text{ Wcm}^{-2}$.
 (a) Relative attenuation of the beam at average laser output powers from 7W to 13 W, corresponding with an intensities of $4\text{-}8 \cdot 10^{19} \text{ Wcm}^{-2}$. (b) Progression of the laser power (black), the broadband plasma emission (red), and the power of the attenuated beam after transmission through the breakdown plasma (blue) for a 1064nm laser pulse with an intensity of $6 \cdot 10^{19} \text{ Wcm}^{-2}$.
 Y-axis: power (not normalized). X-axis: elapsed pulse time 5ns per division.

Fig. 3 shows the recording of the attenuation of a laser beam by the plasma that is generated in air due to the high intensity in the beam focus. The section on the left side shows the relative attenuation of pulsed laser radiation with different average powers. In the right section the laser output powers, the transmission of the laser through the plasma, and the plasma emission are plotted versus the elapsed pulse time. It becomes evident that the fastest declination of the transmission coincides with the fastest inclination of the plasma emission suggesting an especially high absorption of the plasma in its state of advanced excitation. If the plasma is generated from evaporated material enhanced absorption of the laser beam by the plasma and a simultaneous shock wave with its center above the surface of the laser heated solid should occur. The beam should be attenuated and the direct heating of the solid should be reduced [Fig. 4].

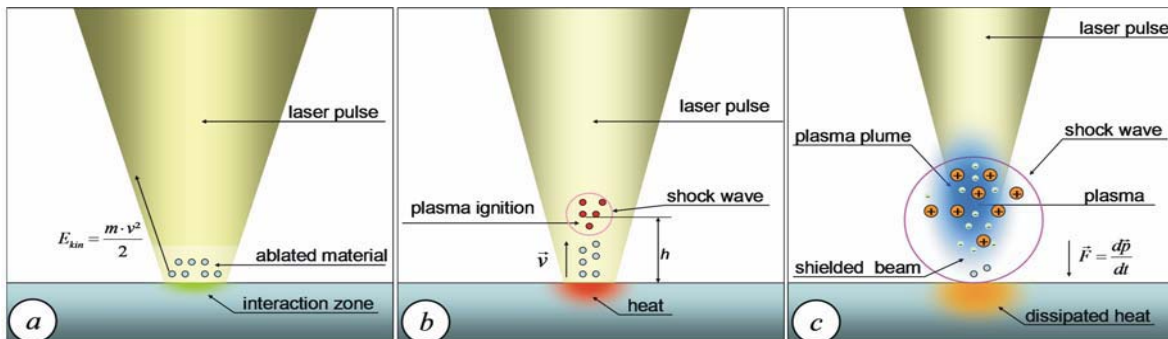


Fig. 4: Schematic of a model with multiple pressure jumps in laser sintering with short and intensive pulses: (a) Vaporous and partially excited material is emitted by the initial direct interaction of the laser beam with the solid. (b) Absorption and attenuation of the laser beam by the vaporous ablation products increase gradually. (c) Enhanced excitation of the plasma effects a pressure jump or shock wave.

Fig. 5 shows a series of high-speed photographs of the pulse effects on a steel substrate. From the expansion of the plume one can estimate the speed of the initially evaporated material as $6 \cdot 10^3 \text{ m s}^{-1}$. If there is a delay between 5-10 ns until enhanced absorption of plasma takes place, as suggested above [Fig. 3], then the plume should have reached a height between 30nm and 100µm. This is a noticeable distance from the position of direct laser-solid interaction.

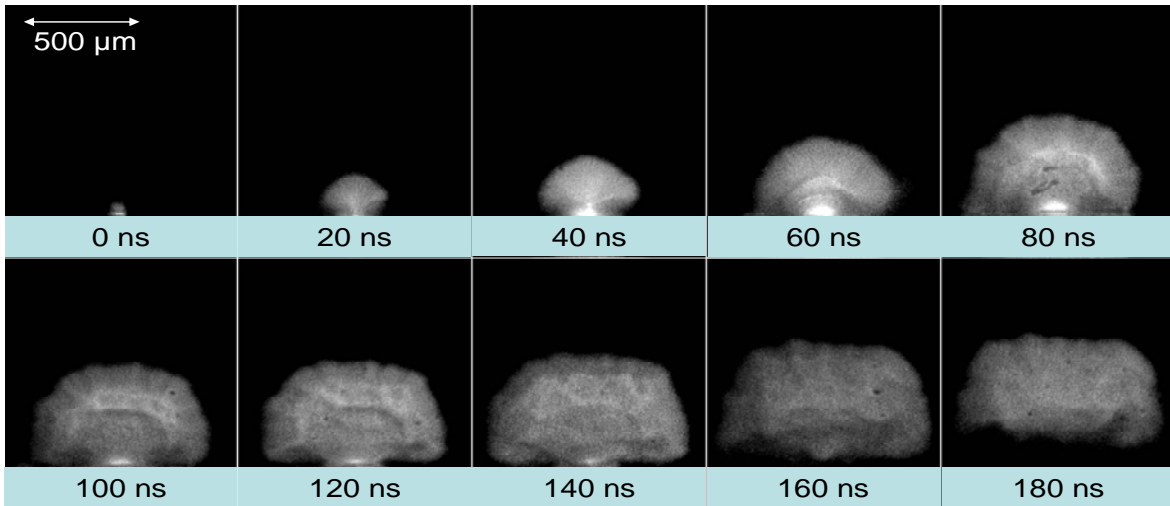


Fig. 5: Plasma expansion during irradiation of steel with a q-switched pulse (90ns, $8 \cdot 10^8$ W/cm²), recorded with a high speed camera (HSFC Pro, PCO AG). The given times are the starting time for reach shot counted from the assumed start of the pulse. Each frame was exposed for 30ns.

In laser micro sintering regimes with pulse lengths of 100-200ns, the repeated occurrence of plasma shock waves in the course of a single pulse could theoretically be expected. In an experiment of the ablation of massive steel with a 90ns pulse, however, a relatively stable plume of residual plasma above the impact position for at least 180 seconds can be observed [Fig. 5] so that repetitive plasma shocks will probably be damped or suppressed by it. Although q-switched pulses are suitable for laser sintering of bodies with a high resolution [Fig. 6b][2] the relatively irregular surface of the fluffy powder layer is still detrimental to the quality of the sintered body. On the one side the plasma shock principally compacts the melting powder and hurls it towards the substrate on the other side, the consistency of the sintering sites for each pulse is different from the other ones: Results of the pulses vary between deep cut-ins through the powder layer and into the substrate material as well as more superficial flattened craters. An extreme example is presented in Fig. 6a.

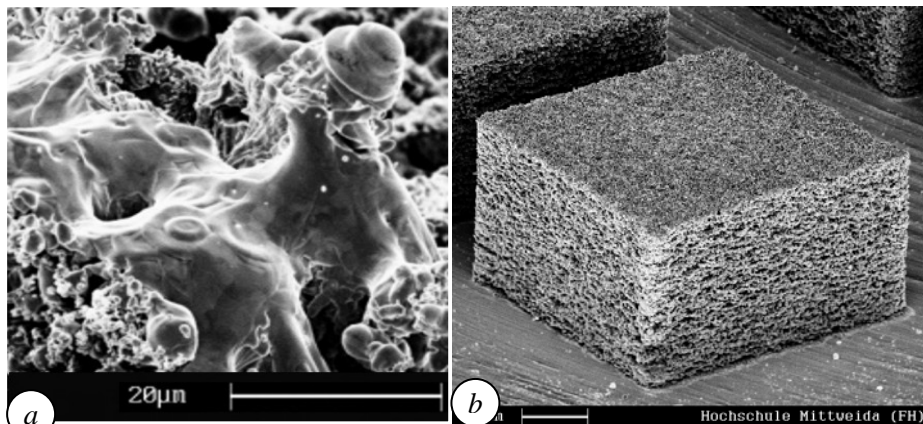


Fig. 6: (a) Typical effects of q-switched pulses on a powder layer; (b) laser micro sintered body from tungsten powder.

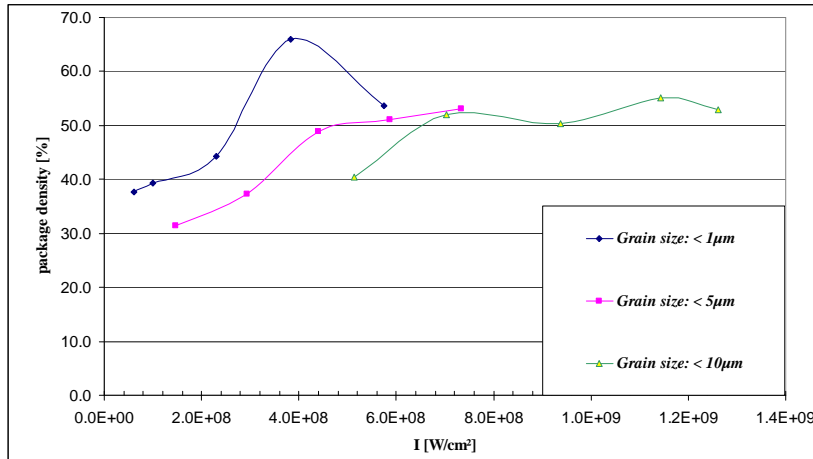


Fig. 7: Relative densities obtained by laser micro sintering of tungsten powders with various grain sizes.

Improvements in powder packing and sinter regimes have led to noticeably regular products already. But, namely in laser micro sintering of metals where the process consists of separated pulse events, the surface texture and roughness still does not reach the quality of a casting. [Fig. 6b]. The relative densities of the sintered bodies from single component powders do not exceed 75% [Fig. 7]. Relative densities of up to 95% were achieved with powder blends of

a refractory and a low melting metal. Higher densities have not been reached yet with - plasma shock supported - laser micro sintering.

Requirements for selective laser sintering of sub-micrometer powders without the aid of plasma shock wave

In selective laser sintering of sub-micrometer powders, the compacting effect of plasma shock waves is one means to avoid the balling of the melt into separate spheres. The limited densities of the bodies achieved with this regime are a significant drawback. It is known that metal melts have a considerably high surface tension. The surface tensions for low-melting metals range around 0.5 Jm^{-2} and for high-melting metals up to 3 Jm^{-2} which is around two orders of magnitude higher than the corresponding value for substances that exist in liquid phase at room temperature.

Laser melting of a 500nm aluminum coating on a glass substrate demonstrates the balling, respectively the contraction by surface tension, of a thin metal layer if fusion to the substrate is not possible. The probe in Fig. 8 was irradiated with single low intensity pulses ($6,8 \cdot 10^6 \text{ W/cm}^2$). The irradiated energy of $6 \mu\text{J}$ per pulse suffices for local melting of the metal layer. The nominal focal diameter was $24 \mu\text{m}$.

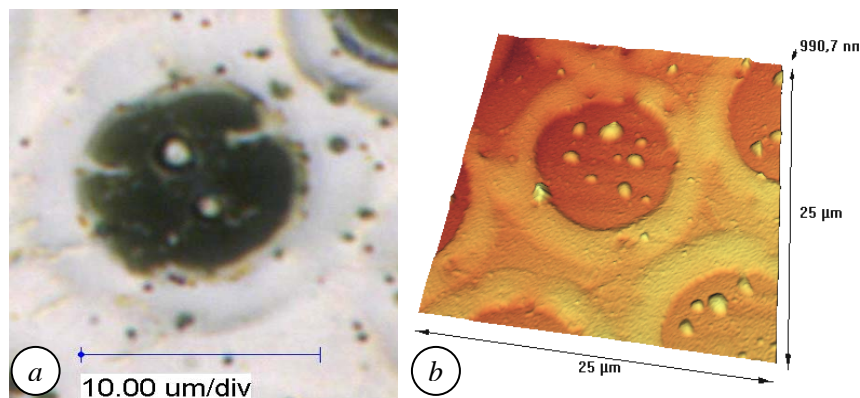


Fig. 8: (a) a laser beam fused aluminum layer on a glass substrate; (b) height-profile from an AFM scan

As expected, the metal that had been molten had contracted almost evenly toward the outside rim of the spot leaving an unmetallized circular area with only a few spherical metal drops. The fusion of the corresponding 14 μm circular section of the aluminum coating affords a minimum intensity of $3 \cdot 10^6 \text{W/cm}^2$.

The comparison with conventional selective laser sintering, where q-switched pulses are not necessary, leads to the consideration if larger drops of molten metal, as they are generated in thicker powder layers, show better wetting properties toward the underlying layer or the substrate, due to the larger deformation (flattening) under the influence of gravity. An estimation of the respective deviation of the a-gravic sphere shape of a liquid metal drop and the resulting size of a flat contact area with the underground as a function of surface tension and specific mass was made. Above a minimum size of this area heat transfer into the substrate should suffice to melt the contact zone of the substrate and allow for mutual wetting and fusion of the melt ball to the underlying body. For the calculation of the size of the contact area second degree inhomogeneous differential equations have to be solved which is not trivial with analytical methods. However, several numerical approaches have been published meanwhile, among others, the method of Runge and Kutta [7]. In this case the Young-Laplace equation [Eq. 1] is applied and solved numerically.

$$\text{Eq. 1} \quad \Delta p = \gamma(k_1 + k_2) = \gamma \left(\frac{1}{r_1} + \frac{1}{r_2} \right) \quad \Delta p - \text{differential pressure, } r - \text{radius}$$

$k - \text{curvature, } \gamma - \text{surface tension}$

Given the specific density and the surface tension as parameters, the surface curvature for a liquid entity under gravity can be calculated as a function of its a-gravic radius. In this relation adhesive effects are neglected; it therefore describes an extreme case of drop deformation.

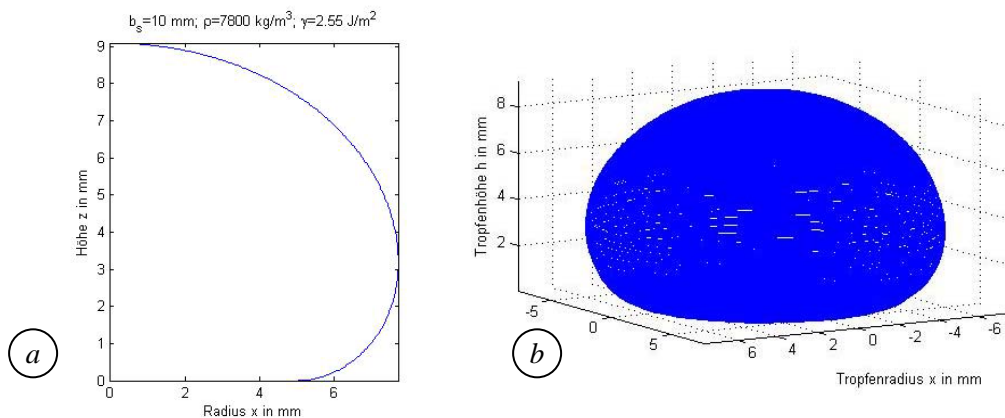


Fig. 9: (a) Cross section view of a gravity deformed bead of liquid steel; diameter of the a-gravic sphere: 10mm (b) 3d-view of the same bead.

Figure 9 shows clearly that even for liquids with a high surface tension drops with a-gravic diameters in the range of several millimeters are flattened considerably by gravity. To get an idea of the order of gravitational deformation for spheres in the micrometer range the radius of the flat contact area versus the radius of the sphere is plotted in Figure 10. According to the computed values the contact radius of liquid aluminum with a surface tension of 1.2 J/m^2 increases almost

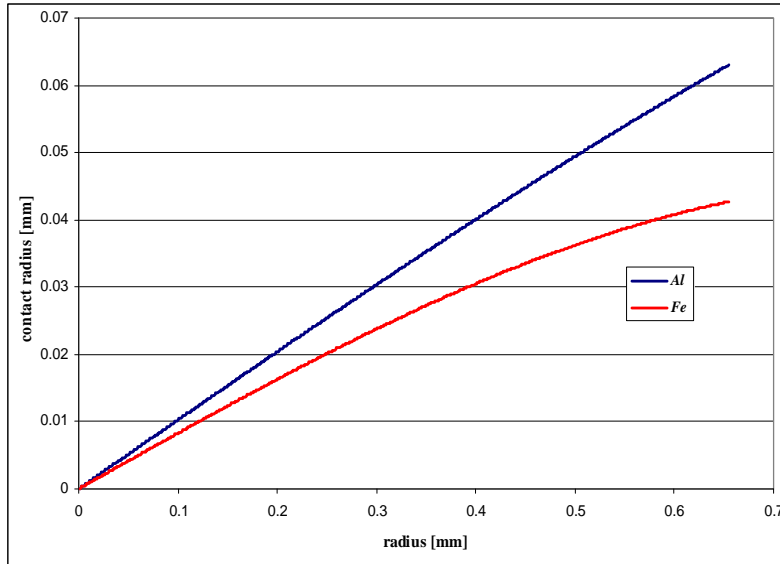


Fig. 10: Contact radius as a function of the agravic drop radius under non-wetting conditions

It seems to be the most reasonable assumption that for successful fusion both, the substrate and the metal drop have to be in liquid state when they get in contact. This implies that in the case of laser sintering sufficient energy has to be transferred to the underlying body for locational melting of the substrate on one hand and for complete melting of the adjacent powder on the other hand.

Sufficient incidence of radiation onto the substrate surface can be achieved when the powder layer is very thin or with appropriately high intensities. With thicker and denser powder layers at the start of each line the laser beam should be attenuated noticeably by the shadowing of the powder. In the further course at constant scan speed a stable hot rim develops around the spot of direct laser incidence, fusing the substrate and part of the powder in this area by thermal heat transfer. Thus high thermal conductivity of the underground material and sufficient contact of the powder with it, promote the performance of laser sintering with a continuous radiation. This entails a high powder packing density from which a correspondingly massive sintered body can be expected with the respective high heat conductivity.

Metal powders of the grain sizes that are suitable for laser micro sintering have relative densities around 20% contrary to those used in conventional selective laser sintering or selective laser melting ($\approx 50\%$) [Fig. 11]. Mechanical compression of the powder layer after coating seems to be the only way to reach the desired higher densities without compacting plasma shock waves.

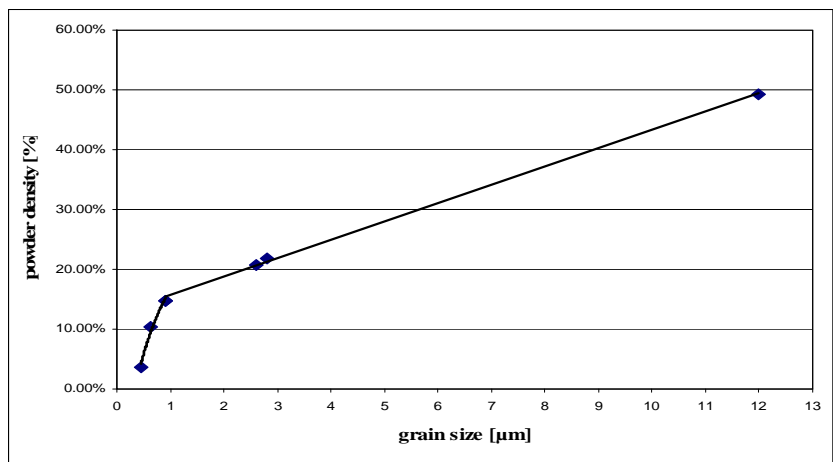


Fig. 11: Relative densities of tungsten powders with different grain sizes.

linearly in the segment of the curve for spherical radii between $1\mu\text{m}$ and $650\mu\text{m}$. In spite of its higher specific mass a drop of iron is deformed much less by gravity due to its higher surface tension of 2.55 J/m^2 .

Anyhow, it can be concluded from the limited contact area that micrometer sized metal drops yield due to gravitational deformation that this very effect is probably of little or no influence for the fusion of a metal drop with its substrate. Also, reported observations show that the wetting behaviour cannot be controlled by the laser parameters alone [4,8,9].

Experimental

For enhancement of the powder coating density a new procedure was introduced. For each coating the probe piston is lowered by the amount of several sinter layers and loaded with powder [Fig. 12a]. The density of the powder in the cylinder above the probe piston is around 20%. The probe cylinder is capped by an external lid, and the powder piston is elevated to its predetermined height compacting the loaded powder by pressing it against the lid [Fig. 12b,c,d]. After compaction the lid is pulled off horizontally [Fig. 12b,e].

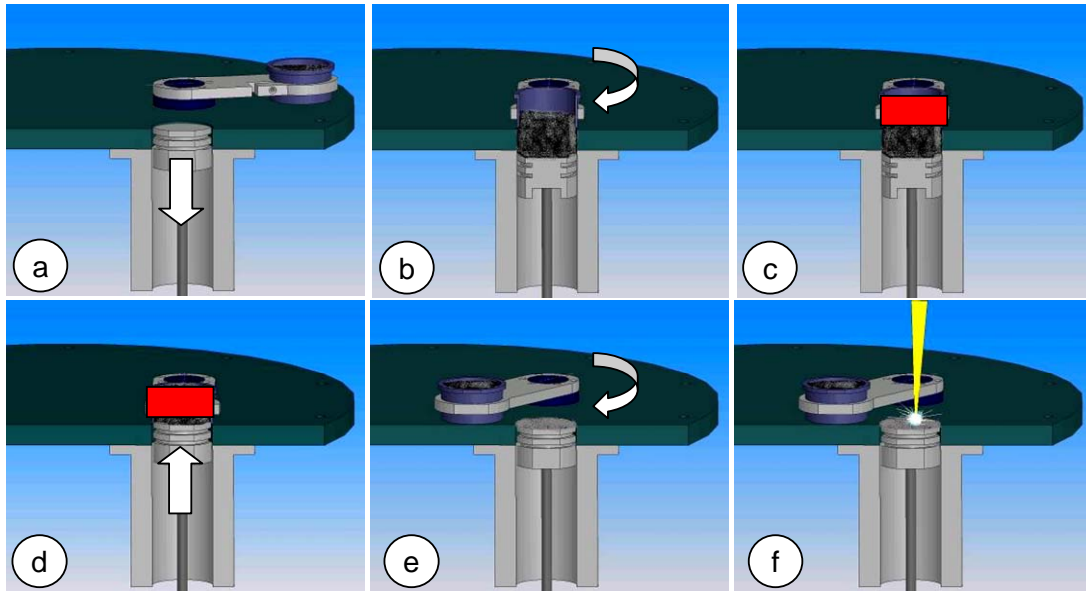


Fig. 12: Procedure of the powder compression (schematic): (a) lowering of the probe platform; (b) loading of the powder (c) capping of the probe cylinder (d) compression of the powder (e) leveling (f) sintering

It was not possible yet to determine the exact quantitative compression since the elastic behavior of the powder is unknown, but estimations yielded compaction ratios between 1.5 and 2.0. The compacting and sinter experiments were performed with molybdenum powder (Alfa Aesar) with a mean grain size of 3.5 μm and a compaction pressure of 5kPa. For the sinter experiments a fiber laser ($\lambda=1064\mu\text{m}$) YLP-C from IPG GmbH Burbach/Germany with a maximum pulse energy of 1mJ and an M^2 of 1.7 was employed. Average powers were used between 0.4W and 5.0W. The beam was focused with an 80mm lens yielding a beam waist diameter of 12.5 μm . The probe was scanned line-wise by the beam such that the sintered sections were filled evenly with the pulses. The distance between adjacent pulses was varied from 4 μm to 20 μm . The intention was to sinter with the lowest possible intensity to exclude plasma shock effects.

Results and discussion

Fig. 13 shows the results of laser sintering of a compressed powder with an average power (p_{av}) of 4.1 W a pulse width of 180 ns, and waist diameter (w_f) of 12.5 μm .

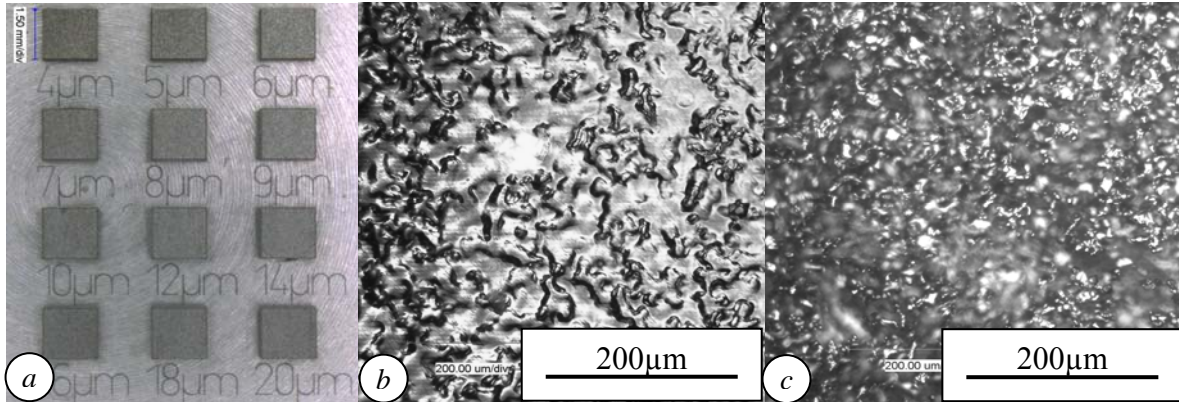


Fig. 13: (a) Matrix of square prisms sintered with varying pulse to pulse distance, ($p_{av}= 4 \text{ W}$; $t_p=180\text{ns}$; $w_f=12.5\mu\text{m}$); (b) surface structure at 5 μm pulse to pulse distance; (c) surface structure at 20 μm pulse to pulse distance.

Contrary to earlier results where the single pulses are clearly visible as stitches in the surface texture of the sintered products [3] the surface of the probes show dense fusion and single pulses cannot be distinguished anymore. Next to the high pulse overlap this is also a consequence of the high heat conductivity of the body. Formerly, with lower powder densities, such a high pulse overlap would have merely caused a high degree of ablation. With increasing pulse to pulse distances heat conduction does not suffice for extensive fusion.

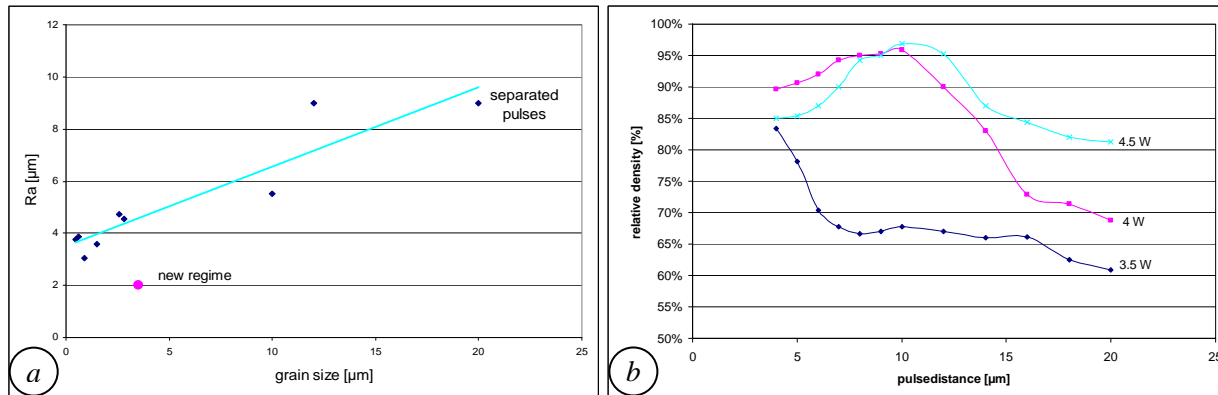


Fig. 14: (a) Sinter-surface roughness R_a vs. grain size resulting from non-compressed (cyan) and compressed (magenta, single value) powder coatings; (b) sinter densities from compressed powder coatings vs. pulse to pulse distance at three different average powers.

Due to the higher degree of fusion the roughness of the sintered bodies is lower [Fig. 14a] and relative sinter densities above 90% can be reached easily [Fig. 14b]. With increasing pulse energy respectively with increasing average power the distance ahead of the laser track, where the temperature is sufficiently high for the preheating, also becomes wider. Therefore, at higher powers, sufficient densities can be obtained although the pulses are placed further apart. Beyond

a certain average power detrimental ablation starts to compete with fusion even under conditions of specially condensed powder layers. In terms of applied energy the highest density (97%) could be achieved with a fluence of 0.5 Jmm^{-2} .

From the high degree of fusion one could expect that, compared to results from sinter regimes with isolated pulses, the resolution of the technique suffers noticeably from collateral heating. Measurements on a demonstrator probe [Fig. 15], however, showed that the oversize of the geometrical features in the sintered product corresponds exactly with the radius of the beam waist which allows the conclusion that because of the effective heat conductance into the sintered body no lateral fusion with non-irradiated powder occurs.

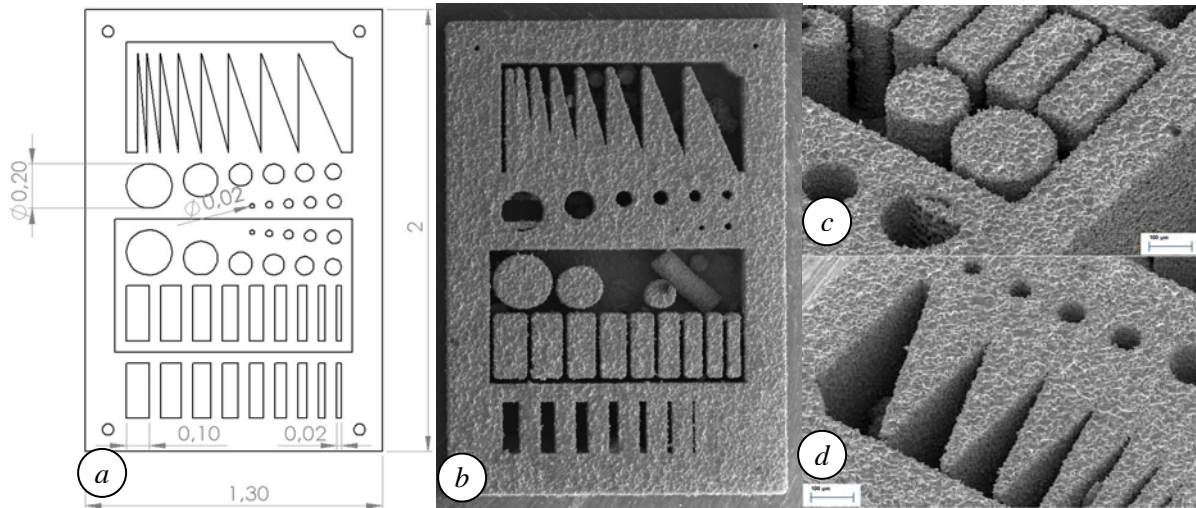


Fig. 15: (a) Sketch of a demonstrator probe for the evaluation of the resolution; (b) total view of the probe; (c)(d) blow-ups of structural details.

To demonstrate the superiority of the described sinter regime a miniaturized turbo charger [Fig. 16] with an outer diameter of 3.5mm was sintered and compared with a sample previously obtained from non-compressed powder with an outer diameter of 12mm and otherwise the same proportions. Fig 16a shows the design drawing of the machine with the detached (for illustrative purposes) coaxial double rotor. Figure 16b shows photographs of both miniatures, each of them was sintered as an entity without any need for subsequent assembly.

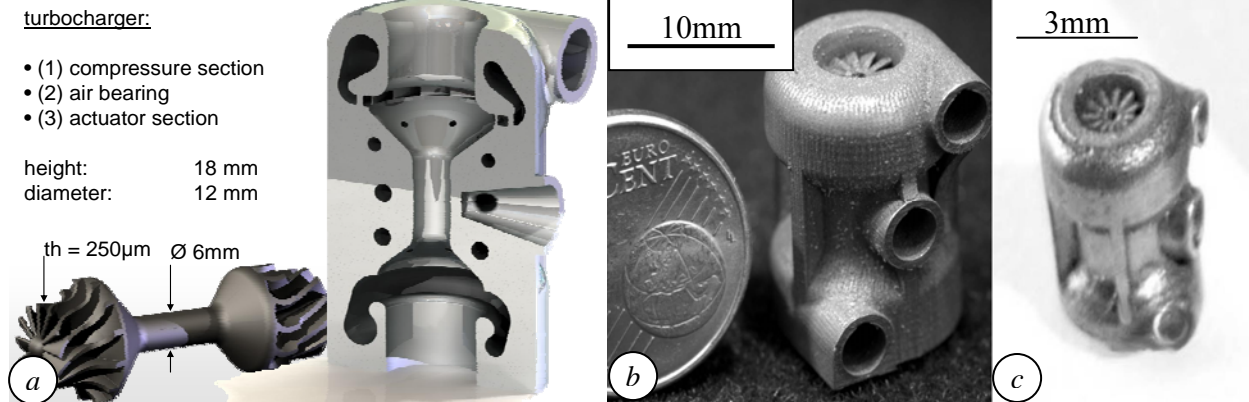


Fig. 16: (a) design drawing of the turbo charger's cross section view; the double rotor of the sintered machines is not detachable. (b) laser micro sintered turbo chargers: with the conventional technique the lower limit were the admeasurements of the construction (c) with compressed powder a 3.5-fold miniaturization could be achieved.

The proper rotation of the turbine with the larger dimensions has been tested already successfully. For the functional test of the smaller one an appropriate method has to be found yet for the removal of the un-sintered powder. Compressed powder layers were crucial for the sintering of the smaller machine. A closer look at the more massive and shiny appearance of its surface indicates the higher density of the body.

Summary

Selective laser sintering of micro-parts from metal powders was heretofore only feasible with a regime of q-switched pulses. This special regime was necessary because of the specific problems that arose from the poor packing of fine grained powders. One of the crucial effects of q-switched laser pulses is the plasma shock wave. An important drawback of the regime is the limited density of the sintered products. Considerations on requirements of fusion without the support of a plasma shock wave led to an approach that is based on the mechanical compression of the powder coating immediately before sintering. The results corroborate the hypothesis that above a minimum powder density fusion of the powder with the substrate is possible without the support of the plasma shock wave. Sinter densities above 90% result from sinter regimes that, when applied to powder layers with lower densities, produce either balling of the powder or cause excessive ablation.

This achievement could be a further step for selective laser sintering of micro parts toward the quality of pressure cast products.

Appreciations

The presented experiments have been funded by 'Bundesministerium für Bildung und Forschung' of Germany in the course of the project 'INNPROFILE – Rapid Microtooling mit laserbasierten Verfahren'. The authors gratefully acknowledge the preparation of the probes and the production of SEM images by Prof. F. Müller and his team, namely A. Eysert and E. Gehrke. Special thanks go to our colleagues J. Schille and Ch. Kujawa for their support with the high speed camera, S. Mauersberger for the measurements of the plasma absorption, T. Süß for the AFM-recordings, and M. Müller for the investigation of the sinter parameters.

References

- [1] Regenfuss, P.; Hartwig, L.; Klötzer, S.; Ebert, R.; Exner, H. (2003):, 'Microparts by a Novel Modification of Selective Laser Sintering'. Conference Paper; Rapid Prototyping and Manufacturing Conference, May 12– 15 2003, Chicago (IL), USA.
- [2] Ebert, R.; Regenfuss P.; Klötzer, S.; Hartwig, L.; Exner, H. (2003), 'Process Assembly for μm -Scale SLS, Reaction Sintering, and CVD', presented at the 4th International Symposium on Laser Precision Microfabrication, June 21-24 2003, Munich, Proceedings of SPI, Vol. 5063, pp. 183-188.
- [3] Regenfuss, P.; Streek, A.; Hartwig, L.; Klötzer, S.; Maaz, A.; Ebert, R.; Exner, H. (2005), 'Advancements in Laser Micro Sintering'. In E. Beyer et al. (Eds): Proceedings of the Third International WLT-Conference on Lasers in Manufacturing 2005, Munich, Germany, June 13-16 2005, ATV-Verlag GmbH, ISBN 3-00-016-402-2, pp. 685-688.
- [4] Kruth J.P.; Froyen, L.; Van Vaerenbergh, J.; Mercelis, J.P.; Rombouts, M.; Lauwers, B. (2004), 'Selective laser melting of iron-based powder', *Journal of Materials Processing Technology* 149 pp. 616–622.
- [5] Fischer, P., Romano, V., Weber, H.P. & Kolossov, S. 2004, 'Pulsed laser sintering of metallic powders', *Thin Solid Films*, vol. 453-454, pp. 139-144.
- [6] Ihlemann, J.; Scholl, A.; Schmidt, H.; Woltf-Rottke, B. (1995) Nanosecond and femtosecond excimer-laser ablation of oxide ceramics, *Appl. Phys. A* 60 pp. 411-417.
- [7] Weiß, G. (2005) 'Numerische Berechnung des Tropfenprofils mit Matlab', retrieved Mai, 13, 2008 from www.math.tu-dresden.de/geo/studenten/Tropfen/Tropfenprofil.pdf.
- [8] Niu, H.J.; Chang, T.H. (1999), 'Instability of scan tracks of selective laser sintering of high speed steel powder', *Scripta Mater.* 41 (11) pp. 1229–1234.
- [9] Hauser, C.; Childs, T:H.C.; Taylor, C.M.; Badrossamay, M. (2003), 'Direct selective laser sintering of tool steel powders to high density. Part A: Effect of laser beam width and scan strategy'. In: D. L. Bourell et al. (Eds): The Proceedings of the 14th Annual SFF Symposium 2003, Austin (TX), USA, pp. 644-655.